A Study about a lunar dome in Palus Putredinis

By Raffaello Lena, Christian Wöhler and George Tarsoudis
Geologic Lunar Research (GLR) group

Abstract

In this study we examine a lunar dome located in Palus Putredinis, termed Putredinis 1. Its diameter corresponds to 7.0±0.5 km and its height to 90±10 m, resulting in a flank slope of 1.47° and an edifice volume of 1.78 km³. According to the inferred spectral, morphometric, and rheologic properties, the dome Putredinis 1 belongs to class C_2 in the GLR classification scheme of effusive domes.

1.Introduction

The mare basins were formed by large impacts which led to large-scale fracturing of the lunar crust. The fractures are commonly interpreted as the conduits along which basaltic magmas ascended to the surface.

Palus Putredinis is a lava-flooded plain bounded by the crater Autolycus to the north and the hills of the Montes Archimedes to the west. The oldest materials visible are those from the impact that produced the Imbrium basin, a multi-ring structure that formed 3.85 billion years ago. The outermost ring is apparent as the mountain range called Montes Apenninus. Multiple inner rings also formed during the impact event, though only the highest points of these are now visible above the later-forming lavas. Examples of such peaks in the north of Mare Imbrium are Montes Spitzbergen and Mons Piton (Wilhelms, 1987). The oldest visible Imbrium lavas are probably those of the lighter albedo plains units inside the main Imbrium ring. They occur between Archimedes and Montes Apenninus, in a region called the Apennine Bench Formation, and are notable for their roughness, lighter color, tectonic features (grabens) and domes.

Lunar domes have formed as effusive shield-like volcanoes or possibly also as laccoliths if the magma remained subsurface (Head and Gifford, 1980; Wöhler and Lena, 2009). A laccolith is a magma intrusion, without effusive process. The

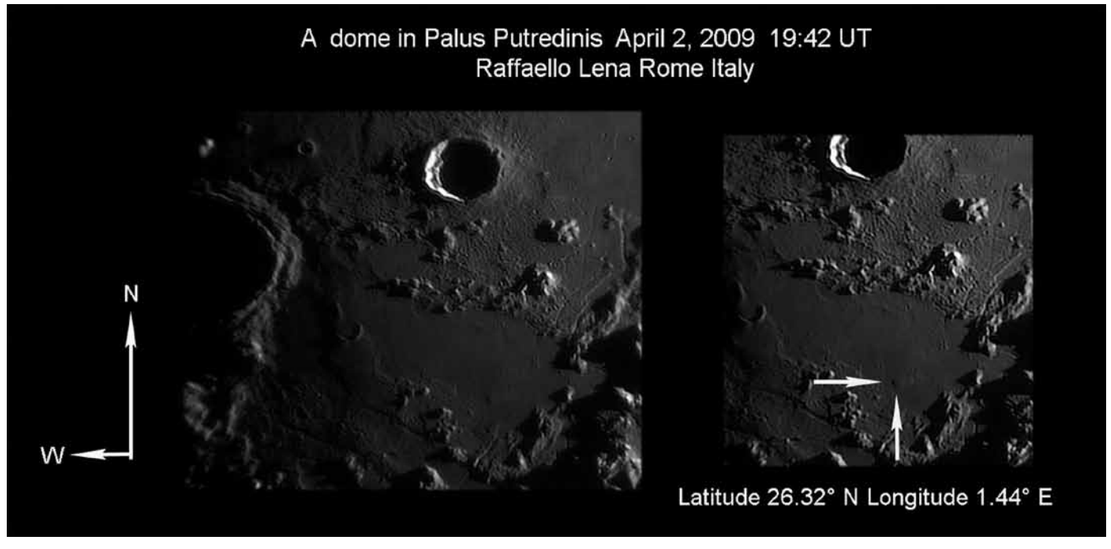

Figure 1: the dome in an image taken by R. Lena on April 2, 2009, at 19:42 UT using a 180 mm Maksutov Cassegrain telescope.

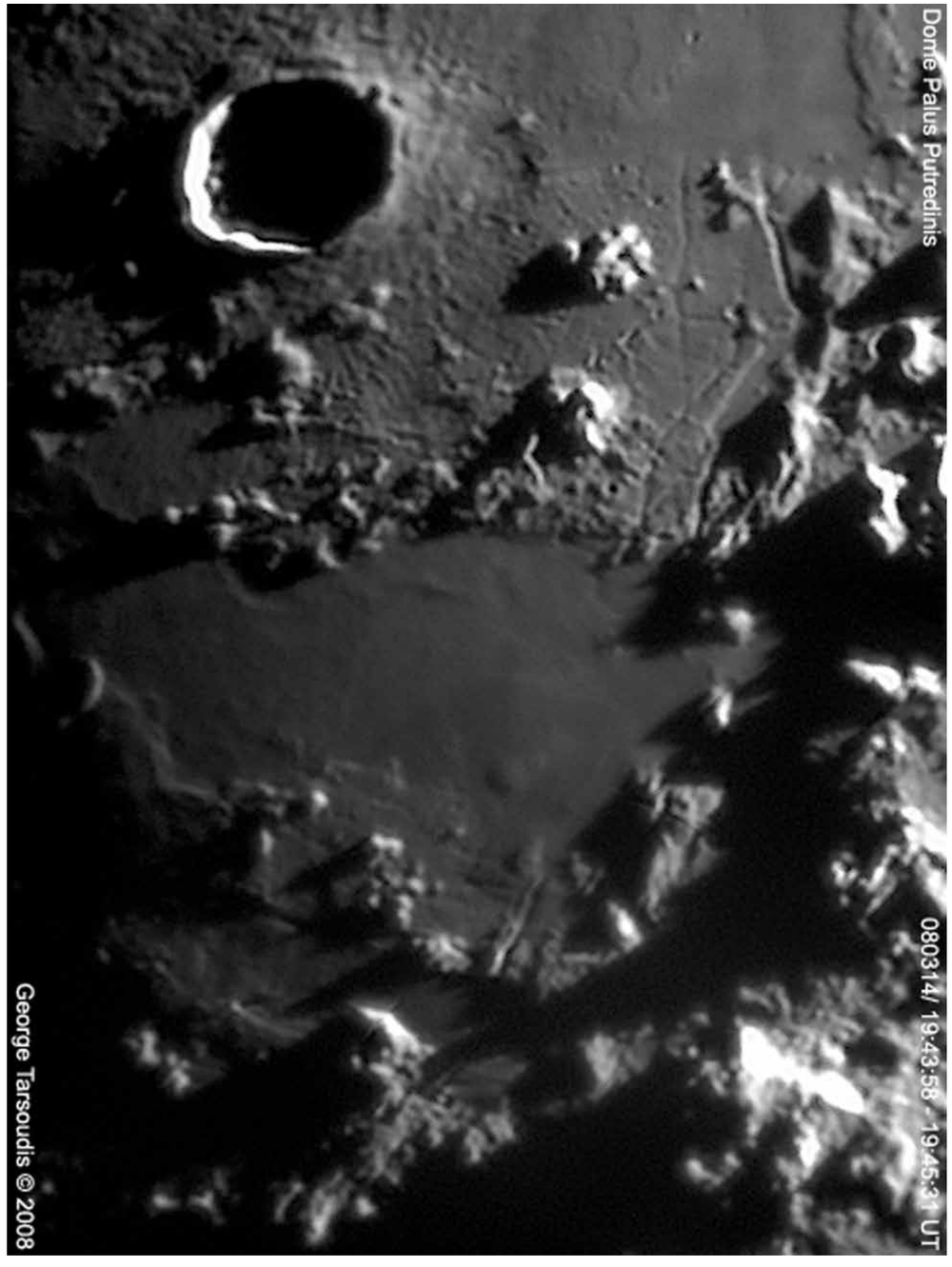

Figure 2: taken by G. Tarsoudis on March 14, 2008 at 19:43 UT using a using a 250 mm Newtonian telescope.

pressure of the magma is high enough that the overlying strata are forced upward, giving the laccolith a dome or mushroom-like form with a generally planar base. These domes are exceptionally large, and most of them are associated with faults or linear rilles of presumably tensional origin. Due to the low profile of domes, Lunar Orbiter and Clementine images do not show domes very well, due to the typically high solar angle on such images. Hence, as part of our program of observing and cataloguing lunar domes, we have used high resolution telescopic CCD images acquired under oblique illumination conditions.

The Consolidated Lunar Dome Catalogue *CLDC* (Lena and Wöhler, 2008) contains all lunar domes which have been studied in detail by the GLR group and for which reasonably accurate morphometric properties could be determined.

In this article we report measurements and include CCD images of a lunar dome located at latitude 26.30°N and longitude 1.44°W in Palus Putredinis, which we have termed Putredinis 1.

2. Method and measurement

For each of the observations, the local solar altitude and the Sun's selenographic colongitude were calculated using the LTVT software package by Mosher and Bondo (2006) which requires a calibration of the images by identifying the precise selenographic coordinates of some landmarks on the image. This calibration was performed based on the UCLN 1994 list of control points. All images are oriented with north to the top and west to the left.

Further morphometric data were obtained by a photoclinometric analysis (Horn, 1989; Carlotto, 1996; Wöhler et al., 2006; Lena et al., 2006 and references therein). We furthermore determined a UVVIS five-band spectrum of the dome based on Clementine imagery at the wavelengths of 415, 750, 900, 950, and 1000 nm. The sample area was 2x2 km^2. The reflectance values were derived relying on the calibrated and normalized Clementine UVVIS reflectance data as provided by Eliason et al. (1999). The extracted Clementine UVVIS data were examined in terms of 750 nm reflectance (albedo) and the R_{415}/R_{750} and R_{950}/R_{750} colour ratios. Albedo at 750 nm is an indicator of variations in soil composition, maturity, particle size, and viewing geometry. The R_{415}/R_{750} colour ratio is essentially a measure for the TiO_2 content of mature basaltic soils, where high R_{415}/R_{750} ratios correspond to high TiO_2 content and vice versa (Charette et al., 1974). However, for many lunar regions the relation between R_{415}/R_{750} ratio and TiO_2 content displays a significant scatter (Gillis and Lucey, 2005). The R_{950}/R_{750} colour ratio is related to the strength of the mafic absorption band, representing a measure of the FeO content of the soil and is also sensitive to the optical maturity of mare and highland materials (Lucey et al. 1998).

3. Telescopic CCD images, spectral, morphometric, and rheologic properties

The shallow dome Putredinis 1 was detected in the images shown in Figs. 1-2. Figure 1 displays the dome in an image taken by R. Lena on April 2, 2009, at 19:42 UT using a 180 mm Maksutov Cassegrain telescope. Another image, shown in Fig. 2, was taken by G. Tarsoudis on March 14, 2008 at 19:43 UT using a using a 250 mm Newtonian telescope.

Further morphometric data were obtained by a photoclinometric analysis. The dome height amounts to 90±10 m, yielding an average flank slope of 1.47°±0.10°. The dome volume V was computed by integrating the reconstructed 3D profile over an area corresponding to a circular region of diameter D around the dome summit. A rough quantitative measure for the shape of the dome is given by the form factor $f = V/[\pi h(D/2)^2]$ (where V=volume, h=height, and D=diameter), where we have f = 1/3 for domes of conical shape, f = 1/2 for parabolic shape, f = 1 for cylindrical shape, and intermediate values for hemispherical shape. For the dome examined in this study, we thus obtain an edifice volume of 1.78 km^3 (f = 0.51). A digital elevation map (DEM) of the region is shown in Fig. 3.

The Clementine UVVIS spectral data of the dome reveal a 750 nm reflectance of R_{750} = 0.07806, a low value of the UV/VIS colour ratio of R_{415}/R_{750} = 0.56338, indicating a low TiO_2 content, and a weak mafic absorption with R_{950}/R_{750} = 1.07864, suggesting a high soil maturity. The rheologic model by Wilson and Head (2003) estimates the yield strength τ (the pressure or stress that must be exceeded for the lava to flow) and the plastic viscosity η, yielding a measure for the fluidity of the erupted lava, the effusion rate E (the lava volume erupted per second) and the duration T of the effusion process. The computed values for τ, η, E, and T are valid for domes that formed from a single flow unit (monogenetic volcanoes). According to the model by Wilson and Head (2003), the yield strength of the dome-forming lava corresponds to τ = 2400 Pa and the viscosity to η = 8.1 x 10^4 Pa s. The lava erupted at an effusion rate of 107 m^3/s over a period of time of 0.53 years (about 28 weeks). To estimate the magma rise speed and the feeder dike geometry, Wilson and Head (2003) apply the dike model by Rubin (1993). Dikes are rising vertical sheets of magma. Rilles often form over rising vertical sheets of magma. A dike can reach the surface and erupt, forming a dome. Based on the estimated lava viscosity and effusion rate, this approach yields a magma rise speed of U = 1.1 x 10^{-4} m/s, a dike width of W = 15 m and a length of L = 67 km.

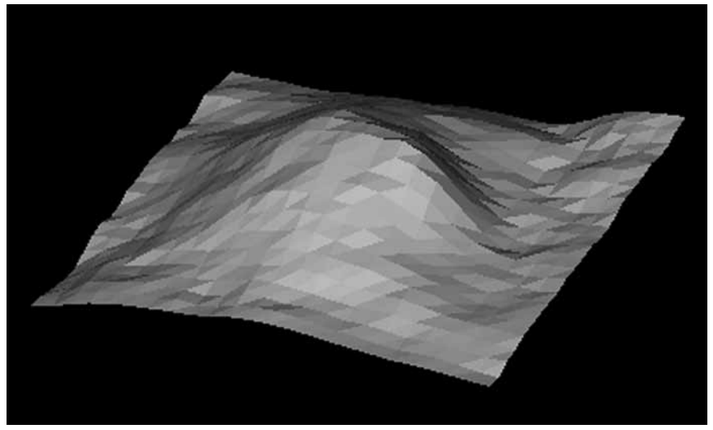

Figure 3: A digital elevation map (DEM) of the region.

4. Result

Based on the spectral and morphometric data obtained in this study, the dome Putredinis 1 belongs to class C_2 in the scheme introduced by Wöhler et al. (2006) and later refined by Lena (2007). It consists of lavas of intermediate to high viscosity and low TiO_2 content, erupting at an intermediate effusion rate. If the effusion of such lava continues over a long period of time, a steep flank slope and high edifice volume may occur as in the case of Archytas 2, which belongs to class B_1, while short durations of the effusion process result in lower and less voluminous edifices, as is the case for domes of class B_2 such as the dome H7 near the crater Hortensius (Wöhler et al, 2006; Wöhler et al, 2007; Lena et al, 2007; Lena et al, 2008).

Wöhler et al. (2007) establish three rheologic groups of effusive lunar mare domes. The first group, R_1, is characterised by lava viscosities of 10^4–10^6 Pa s, magma rise speeds of 10^{-5}–10^{-3} m/s, dike widths around 10–30 m, and dike lengths between about 30 and 200 km. Rheologic group R_2 is characterised by low lava viscosities between 10^2 and 10^4 Pa s, fast magma ascent (U > 10^{-3} m s^{-1}), narrow (W = 1–4 m) and short (L = 7–20 km) feeder dikes. The third group, R3, is made up of domes which formed from highly viscous lavas of 10^6–10^8 Pa s, ascending at very low speeds of 10^{-6}–10^{-5} m s^{-1} through broad dikes of several tens to 200 m width and 100–200 km length. According to the rheologic properties inferred for the dome Putredinis 1, it clearly belongs to rheologic group R_1 like several domes in the Milichius/T. Mayer region and the well-known domes Cauchy τ and ω in Mare Tranquillitatis.

References

[1] Carlotto, M.J., 1996. Shape From Shading. *http://www.newfrontiersinscience.com/martianenigmas/Articles/SFS/sfs.html*

[2] Charette, M. P., McCord, T. B., Pieters, C. M., Adams, J. B., 1974. Application of remote spectral

reflectance measurements to lunar geology classification and determination of titanium content of lunar soils. *J. Geophys. Res*. 79, 1605-1613.

[3] Eliason, E., Isbell, C., Lee, E., Becker, T., Gaddis, L., McEwen, A., Robinson, M., 1999. Mission to the Moon: the Clementine UVVIS global mosaic. *PDS Volumes USA NASA PDS CL 4001 4078. http://pdsmaps.wr.usgs.gov*

[4] Gillis, J. J., Lucey, P. G., 2005. Evidence that UVVIS ratio is not a simple linear function of TiO_2 content for lunar mare basalts. *Lunar Planet. Sci. XXXVI*, abstract #2252.

[5] Head, J., Gifford, A., Lunar mare domes: classification and modes of origin, The Moon and Planets, 22, 1980.

[6] Horn, B. K. P., 1989. Height and Gradient from Shading, MIT technical report, AI memo no. 1105A. *http://people.csail.mit.edu/people/bkph/AIM/AIM-1105A-TEX.pdf*

[7] Lena, R., Wöhler, C., Bregante, M. T., Fattinnanzi, C., 2006. A combined morphometric and spectrophotometric study of the complex lunar volcanic region in the south of Petavius. *Journal of the Royal Astronomical Society of Canada* 100(1), pp. 14-25.

[8] Lena, R., Wöhler, C., Phillips, J., Wirths, M., Bregante, M.T. 2007. Lunar domes in the Doppelmayer region: Spectrophotometry, morphometry, rheology, and eruption conditions. *Planetary and Space Science*, vol. 55, 1201-1217.

[9] Lena, R., Wöhler, C., Bregante, M.T, Lazzarotti, P., Lammel, S., 2008. Lunar domes in Mare Undarum: Spectral and morphometric properties, eruption conditions, and mode of emplacement. *Planetary and Space Science*, vol. 56, 3-4, pp. 553-569.

[10] Lena, R., Wöhler, C., 2008. Consolidated Lunar Dome Catalogue (CLDC). *http://digilander.libero.it/glrgroup/consolidatedlunardomecatalogue.htm*

[11] Lucey, P. G., Blewett, D. T., Hawke, B. R., 1998. Mapping the FeO and TiO2 content of the lunar surface with multispectral imagery, J. *Geophys. Res.*, vol. 103, no. E2, pp. 3679-3699.

[12] Mosher, J., Bondo, H., 2006. Lunar Termination Visualization Tool (LTVT). *http://inet.uni2.dk/ d120588/henrik/jim ltvt.html*

[13] Rubin, A. S., 1993. Dikes vs. diapirs in viscoelastic rock. *Earth and Planet. Sci.* Lett. 199, pp. 641-659.

[14] Wilhelms, D., The Geologic History of the Moon, USGS Prof. Paper 1348. Washington: GPO, 1987.

[15] Wilson, L., Head, J. W., 2003. Lunar Gruithuisen and Mairan domes: Rheology and mode of emplacement, *J. Geophys. Res.* 108(E2), pp. 5012-5018.

[16] Wöhler, C., Lena, R., Lazzarotti, P., Phillips, J., Wirths, M., Pujic, Z., 2006. A combined spectrophotometric and morphometric study of the lunar mare dome fields near Cauchy, Arago, Hortensius, and Milichius. *Icarus* 183(2), pp. 237-264.

[17] Wöhler, C., Lena, R., Phillips, J. Formation of lunar mare domes along crustal fractures: Rheologic conditions, dimensions of feeder dikes, and the role of magma evolution. Icarus, vol. 189, no. 2, pp. 279-307, 2007.

[18] Wöhler, C., Lena, R., 2009. Lunar intrusive domes: Morphometric analysis and laccolith modelling. *Icarus*, in press.

The Photography of Richard Hill